Electronic Supplementary Information

Influence of Interfacial Water and Cations on the Oxidation of CO at the Platinum/Ionic Liquid Interface

*Björn Ratschmeier, Gina Ross, Andre Kemna and Björn Braunschweig**

Institute of Physical Chemistry, Westfälische Wilhelms-Universität Münster, Corrensstraße 28/30, 48149 Münster, Germany

*braunschweig@uni-muenster.de

Reference Electrode Calibration and Pt(111) Surface Characterization

Due to its distinct redox couple, the use of ferrocene/ferrocenium (Fc/Fc^+) as an internal standard is a widespread method (Figure S1a). For the calibration of the Ag/Ag^+ reference electrode, we used a Pt working and a Pt counter electrode in a three-electrode configuration with 2.5 mM ferrocene which was dissolved into the corresponding RTIL. The redox potential was calculated by $E_{1/2} = 1/2(E_{pa} + E_{pc})$ vs Ag/Ag^+ of the redox couple. The conversion to SHE as a reference system was made as described previously by Pavlishchuk et al.[1] using a conversion constant of +624 mV from Fc/Fc^+ to SHE. The resulting reference potentials are used by assuming that all RTILs in our study are similar in acetonitrile and the results are summarized below in Table S1.

To verify the (111) orientation of the Pt(111) electrode and the surface quality, we have recorded a cyclic voltammogram (CV) in a 0.5 M H_2SO_4 aqueous electrolyte after preparation of the electrode which was done as reported in the main text. The corresponding CV of a well-ordered Pt(111) electrode is shown in Figure S1b. Noticeable is the plateau region up to 0.2 V, representing hydrogen under potential deposition (UPD) and hydrogen stripping for cathodic and anodic cycles, respectively.[2] The narrow peaks are caused by a low density of defects with (100) and (110) orientation which are unavoidable when large single crystals (here 10 mm in diameter) are used.[3] Sulfate adsorption and desorption, respectively, are attributable to the current wave between 0.3 and 0.45 V, with the pronounced sharp feature at 0.45 V that is due to an order-disorder transition from a disordered (bi)sulfate adlayer to an ordered closed-packed $(\sqrt{3}\times\sqrt{7})R19.1°$ superstructure of (bi)sulfate.[4–6] The sharpness of this feature is indicative of long-range surface order and shows that we are able to prepare a clean Pt(111) electrode with a low density of defects.[6] In addition, the features between 0.6 and 0.8 V are associated with OH ad- and desorption, respectively.[7,8]

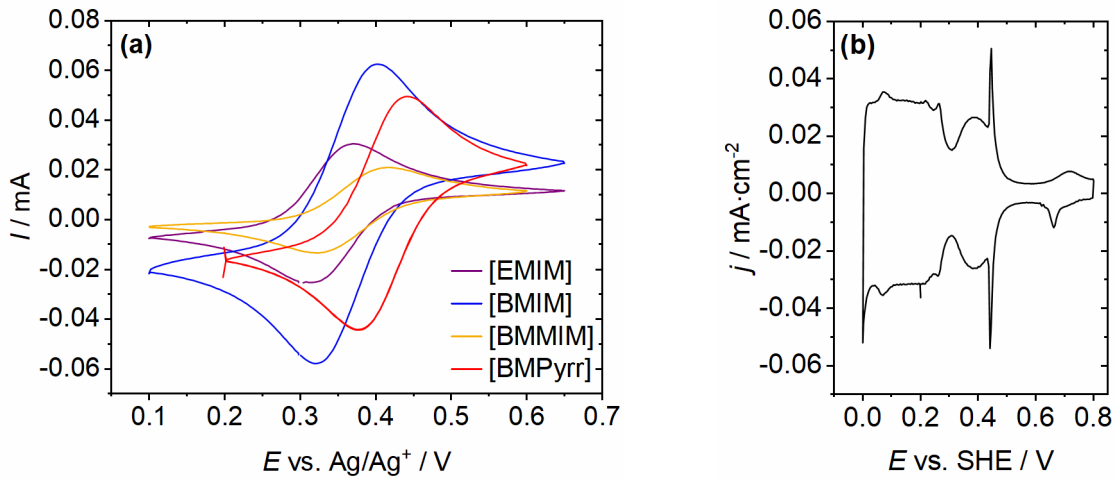

Fig. S1. *(a) Cyclic voltammograms (20th cycle) of 2.5 mM ferrocene dissolved in [EMIM], [BMIM], [BMMIM] and [BMPyrr][NTf₂] with a Pt working and counter electrode and Ag/Ag⁺ reference electrode measured under Ar saturation and at a sweep rate of 50 mV/s. (b) Cyclic voltammogram of Pt(111) in Ar saturated 0.5 M H_2SO_4 measured at 50 mV/s in a hanging meniscus configuration.*

Table S1. *Redox potential of the redox couple Fc/Fc⁺ measured in different RTIL reported in Figure S1a. The potentials are converted with conversion constant of +624 mV from Fc/Fc⁺ to SHE according to Pavlishchuk et al.*[1]

RTIL	*E* (Fc/Fc⁺ vs. Ag/Ag⁺)	*E* (Ag/Ag⁺ vs. SHE)
[EMIM][NTf₂]	343 mV	281 mV
[BMIM][NTf₂]	361 mV	263 mV
[BMMIM][NTf₂]	370 mV	254 mV
[BMPyrr][NTf₂]	410 mV	214 mV

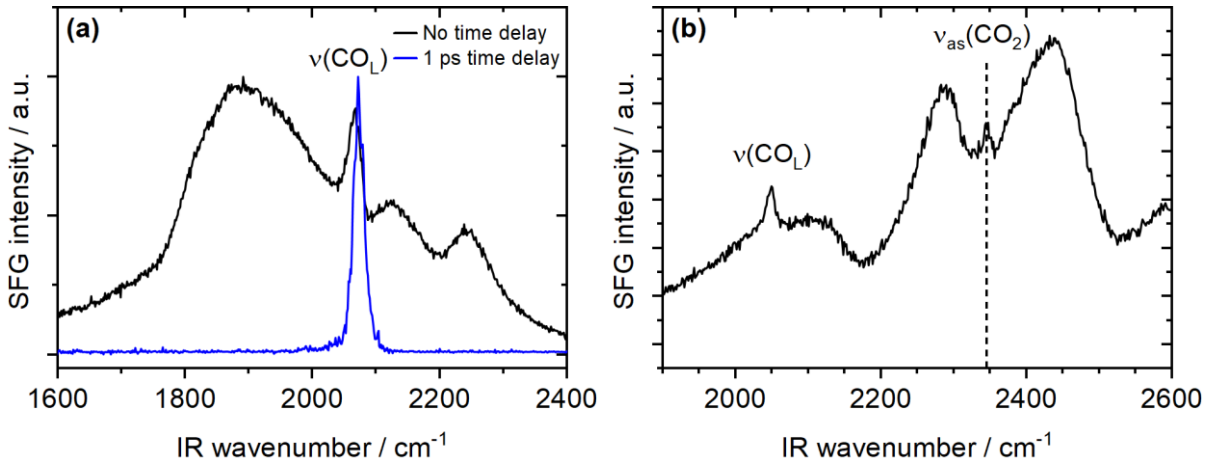

Fig. S2. *(a) SFG spectrum of the Pt(111)/[BMIM][NTf₂] interface with 10 mM H_2O and pre-adsorbed CO under N_2 saturation of the electrolyte at 0.1 V vs. SHE. The non-resonant contribution gets suppressed by adding a 1 ps time-delay for the VIS pulse. (b) SFG spectrum without time delay of the Pt(111)/[BMIM][NTf₂] interface with 10 mM H_2O at 0.1 V vs. SHE showing the CO_2 antisymmetric stretching vibrational band of atmospheric CO_2, which is used for $\nu(CO_L)$ calibration.*

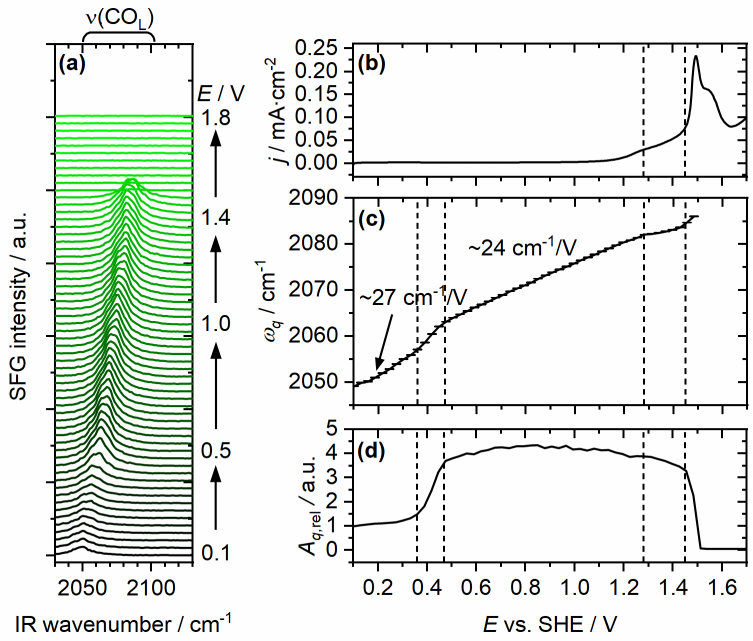

Fig. S3. *(a) In situ SFG spectra of the Pt(111)/[EMIM][NTf$_2$] interface with 0.5 M H$_2$O and pre-adsorbed CO under N$_2$ saturation at a sweep rate of 5 mV/s. (B) Voltammogram of the Pt(111)/[EMIM][NTf$_2$] interface and pre-adsorbed CO under Ar saturation measured in a hanging meniscus configuration at 50 mV/s. (c)/(d) Frequency and amplitude change of the CO$_L$ band in (a), which are obtained by fitting the spectra with a Lorentzian function according to equation (1).*

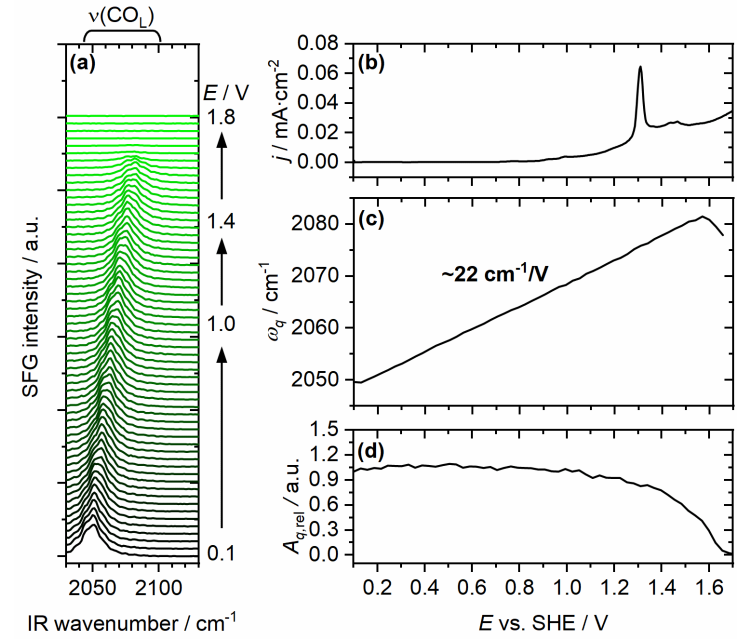

Fig. S4. *(a) In situ SFG spectra of the Pt(111)/[BMMIM][NTf$_2$] interface with 0.5 M H$_2$O and pre-adsorbed CO under N$_2$ saturation at a sweep rate of 5 mV/s. (B) Voltammogram of the Pt(111)/[BMMIM][NTf$_2$] interface and pre-adsorbed CO under Ar saturation measured in a hanging meniscus configuration at 50 mV/s. (c)/(d) Frequency and amplitude change of the CO$_L$ band in (a), which are obtained by fitting the spectra with a Lorentzian function according to equation (1).*

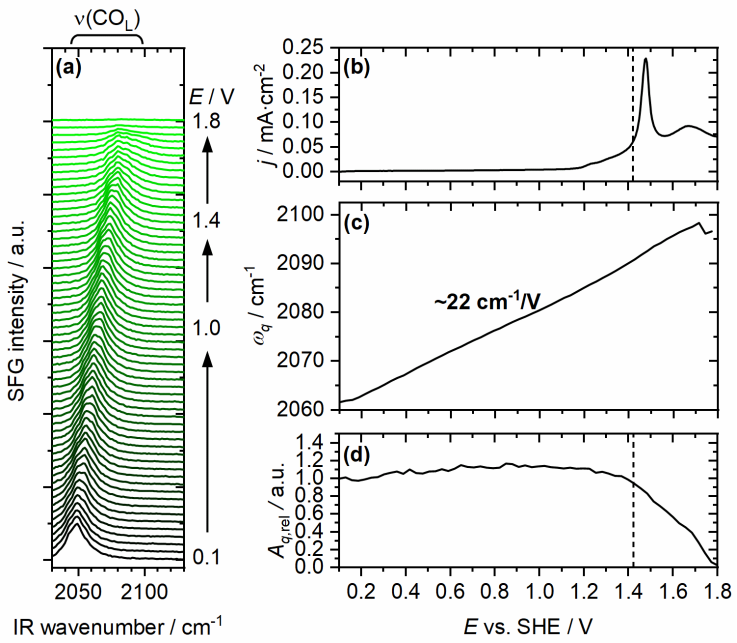

Fig. S5. *(a) In situ SFG spectra of the Pt(111)/[BMPyrr][NTf$_2$] interface with 0.5 M H$_2$O and pre-adsorbed CO under N$_2$ saturation at a sweep rate of 5 mV/s. (B) Voltammogram of the Pt(111)/[BMPyrr][NTf$_2$] interface and pre-adsorbed CO under Ar saturation measured in a hanging meniscus configuration at 50 mV/s. (c)/(d) Frequency and amplitude change of the CO$_L$ band in (a), which are obtained by fitting the spectra with a Lorentzian function according to equation (1).*

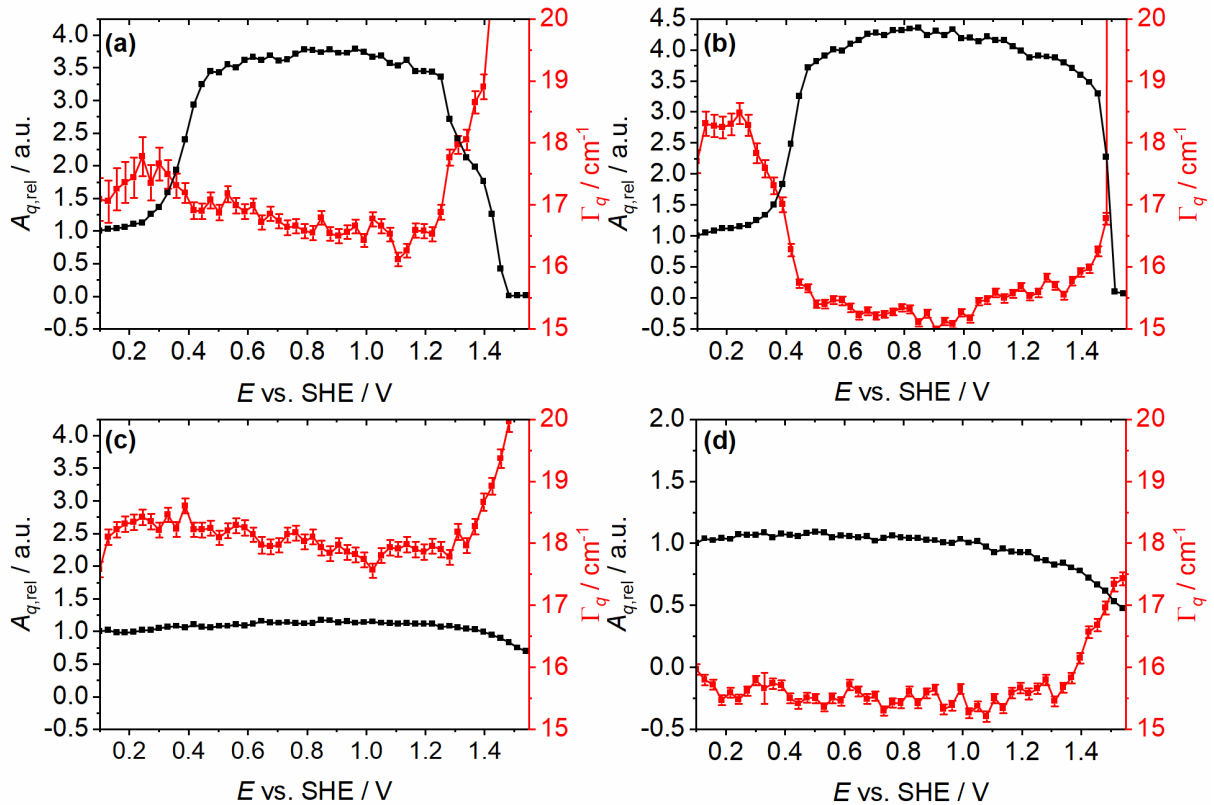

Fig. S6. *Amplitude and bandwidth change of the CO$_L$ band at the Pt(111)/(a) [BMIM], (b) [EMIM], (c) [BMIM] and (d) [BMPyrr][NTf$_2$] interface with a H$_2$O concentration of 0.5 M, which are obtained by fitting the corresponding SFG spectra with a Lorentzian function according to equation (1).*

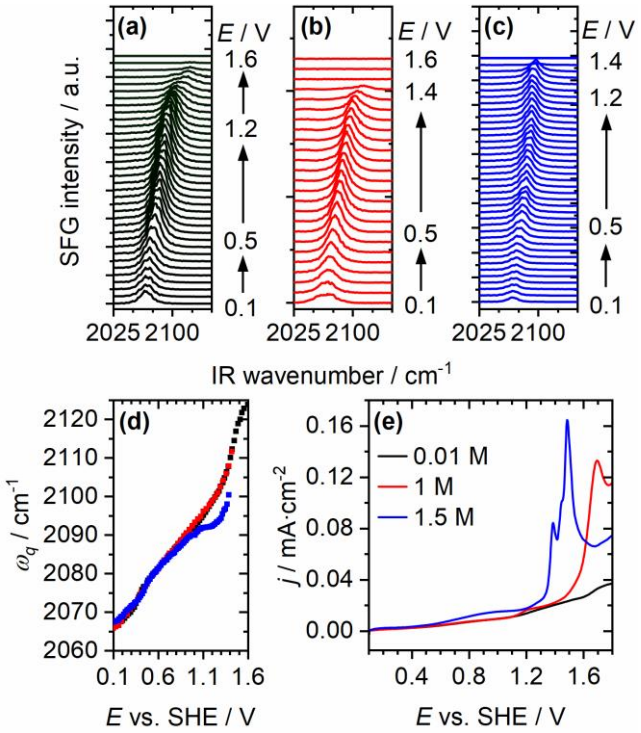

Fig. S7. *In situ SFG spectra of the Pt(111)/[BMIM][NTf_2] interface with (a) 0.01 M (b) 1 M and (c) 1.5 M H_2O and pre-adsorbed CO while the electrolyte was saturated with N_2. The sweep rate was set to 5 mV/s, while SFG were recorded synchronized to the change in electrode potential. (d) Frequency change of the CO_L band for different water concentrations which were generated by fitting the SFG spectra with a Lorentzian function according to equation (1). (e) Voltammograms of the Pt(111)/[BMIM][NTf_2] interfaces with different H_2O concentrations as indicated in the Figure and pre-adsorbed CO when saturated with Ar. CV were measured in a hanging meniscus configuration with a sweep rate of 50 mV/s.*

References

(1) Pavlishchuk, V. V.; Addison, A. W. Conversion Constants for Redox Potentials Measured Versus Different Reference Electrodes in Acetonitrile Solutions at 25°C. *Inorg. Chim. Acta* **2000**, *298* (1), 97–102.

(2) Braunschweig, B.; Wieckowski, A. Surface Spectroscopy of Pt(1 1 1) Single-Crystal Electrolyte Interfaces with Broadband Sum-Frequency Generation. *J. Electroanal. Chem.* **2014**, *716*, 136–144.

(3) Kibler, L.A.; Cuesta, A.; Kleinert, M.; Kolb, D.M. In-Situ STM Characterisation of the Surface Morphology of Platinum Single Crystal Electrodes as a Function of Their Preparation. *J. Electroanal. Chem.* **2000**, *484* (1), 73–82.

(4) Braunschweig, B.; Daum, W. Superstructures and Order-Disorder Transition of Sulfate Adlayers on Pt(111) in Sulfuric Acid Solution. *Langmuir* **2009**, *25* (18), 11112–11120.

(5) Funtikov, A. M.; Stimming, U.; Vogel, R. Anion Adsorption From Sulfuric Acid Solutions on Pt(111) Single Crystal Electrodes. *J. Electroanal. Chem.* **1997**, *428* (1-2), 147–153.

(6) Clavilier, J.; Rodes, A.; Achi, K. E.; Zamakhchari, M. A. Electrochemistry at Platinum Single Crystal Surfaces in Acidic Media : Hydrogen and Oxygen Adsorption. *J. Chim. Phys.* **1991**, *88*, 1291–1337.

(7) García, N.; Climent, V.; Orts, J. M.; Feliu, J. M.; Aldaz, A. Effect of pH and Alkaline Metal Cations on the Voltammetry of Pt(111) Single Crystal Electrodes in Sulfuric Acid Solution. *ChemPhysChem* **2004**, *5* (8), 1221–1227.
(8) Saravanan, C.; Koper, M. T. M.; Markovic, N. M.; Head-Gordon, M.; Ross, P. N. Modeling Base Voltammetry and CO Electrooxidation at the Pt(111)-Electrolyte Interface: Monte Carlo Simulations Including Anion Adsorption. *Phys. Chem. Chem. Phys.* **2002**, *4* (12), 2660–2666.